Accepted Manuscript

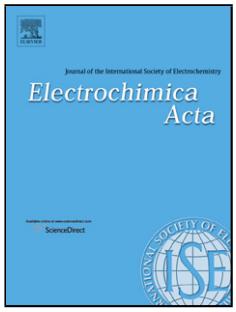

Title: Electrochemical and spectrophotometric characterisation of protein kinase inhibitor and anticancer drug danusertib

Author: Oana M. Popa Victor C. Diculescu

PII: S0013-4686(13)01739-8
DOI: http://dx.doi.org/doi:10.1016/j.electacta.2013.09.017
Reference: EA 21234

To appear in: *Electrochimica Acta*

Received date: 30-7-2013
Revised date: 2-9-2013
Accepted date: 2-9-2013

Please cite this article as: O.M. Popa, V.C. Diculescu, Electrochemical and spectrophotometric characterisation of protein kinase inhibitor and anticancer drug danusertib, *Electrochimica Acta* (2013), http://dx.doi.org/10.1016/j.electacta.2013.09.017

Electrochemical and spectrophotometric characterisation of protein kinase inhibitor and anticancer drug danusertib

Oana M. Popa[1,2] and Victor C. Diculescu[1]*

1 Departamento de Engenharia Mecânica, Faculdade de Ciências e Tecnologia, Universidade de Coimbra, Rua Luís Reis Santos, 3030-788 Coimbra, Portugal

2 Faculty of Physics, University of Bucharest, 077125 Magurele-Bucharest, Romania

*To whom correspondence should be addressed
Phone/Fax: +351 239 700 943/912
Email: victorcd@ipn.pt
Instituto Pedro Nunes
Laboratório de Electroanálise e Corrosão
Rua Pedro Nunes
3030-199, Coimbra, Portugal

Abstract

The electrochemical oxidation mechanism of the anti-cancer drug and kinases inhibitor danusertib was studied by cyclic, differential pulse, square wave voltammetry and a glassy carbon electrode. Danusertib undergoes oxidation in a cascade mechanism and depending on the pH of the supporting electrolyte several oxidation peaks were observed. The number of electrons and protons involved in each oxidation step as well as the pK_a ~ 10.0 were determined. The analytical determination of danusertib was carried out in pH = 7.0 by square wave voltammetry with LOD = 27.4 nM and UV-VIS spectrophotometry with LOD = 0.5 μM. Different electroactive centres of danusertib were identified through comparative studies with similar compounds such as imatinib and piperazine, and an oxidation mechanism of danusertib proposed.

Keywords: danusertib; kinase inhibitor; glassy carbon; redox mechanism; analytical determination.

1 Introduction

Protein kinases represent a major class of enzymes that play an important role in signal transduction pathways, regulating a number of cellular functions such as cell growth, differentiation and cell death [1,2]. Aurora kinases are serine/threonine kinases essential for mitosis, cytokinesis and deregulated chromosome segregation [3] and are overexpressed in many malignancies, including pancreatic, colorectal, ovarian, and oesophageal cancer [4].

In view of the critical role that kinases play in cellular environment, and their overexpression in tumour cells, enzyme kinases were considered excellent targets for anticancer therapy [5]. Several kinase inhibitors were developed and their potential against various cancers have been described during different phases of treatment [6,7].

Danusertib (formally PHA-739358) [8,9], Scheme 1A, is a new, small ATP competitive molecule that inhibits Aurora kinases *in vitro* and *in vivo* [10]. Also, danusertib binds and inhibits with high affinity ($IC_{50} < 0.50$ μM) several other tyrosine kinases such as Abl, Ret, FGFR-1 and TrkA which are involved in the pathogenesis of a variety of cancers [11]. The cross-reactivity of danusertib with different receptor kinases has great anticancer therapeutic potential [12], turning this drug effective for the treatment of multiple tumour models [4].

Clinical trials for the determination of danusertib efficacy in treatment of prostate [13], gastroenteropancreatic [14], hepatic [15], and haematological [16] malignancies have shown a favourable pharmacokinetic and safety profile. Despite the positive results, resistance to danusertib treatment emerged during several studies, but its ability in producing molecular complete remissions of tumours was improved using combinations with traditional anti-neoplastic agents [17].

Being a relatively new drug, most references in the specialized literature deal with clinical studies. The crystal structure of the Abl kinase mutant in complex with danusertib has been resolved and the mechanism by which danusertib may be used to treat resistant leukaemia cells explained [18]. However, considering the importance of danusertib as a chemotherapeutic agent, suitable analytical procedures are required so that issues such as drug-drug or drug-biomolecular complex interactions can be evaluated.

Electroanalytical methods are fast, inexpensive, and the investigation of the electrochemical oxidation mechanisms of compounds has the potential for providing valuable insights into their biological redox reactions. Electroanalysis has been successfully used to determine the redox mechanism of several pharmaceutical compounds and to quantitate different types of drugs [19-24].

In this context, the aim of the present study is the investigation of the electron transfer properties of danusertib using a glassy carbon electrode and electrochemical techniques, cyclic, differential pulse and square wave voltammetry. In order to understand and explain danusertib redox reactions, its electrochemical behaviour was compared with chemical analogues such as imatinib mesylate, Scheme 1B, and piperazine citrate. The analytical determination of danusertib had been also carried by voltammetry and UV-VIS spectrophotometry.

2 Experimental

2.1 Materials and reagents

Danusertib from Selleck Chemicals, imatinib mesylate from Novartis (Portugal) and piperazine citrate from Merck were used without purification. All supporting electrolyte solutions, Table 1, were prepared using analytical grade reagents and purified water from a Millipore Milli-Q system (conductivity ≤ 0.1 μS cm^{-1}). Stock solutions of 5 mM danusertib

and 1 mM imatinib mesylate in ethanol and 1 mM piperazine citrate in deionised water were kept at +4 °C until further utilisation. Solutions of different concentrations of danusertib, imatinib mesylate and piperazine citrate were obtained by dilution of the appropriate volume in supporting electrolyte.

Microvolumes were measured using EP-10 and EP-100 Plus Motorized Microliter Pippettes (Rainin Instrument Co. Inc., Woburn, USA). The pH measurements were carried out with a Crison micropH 2001 pH-meter with an Ingold combined glass electrode. All experiments were done at room temperature (25±1°C).

2.2 Voltammetric parameters and electrochemical cells

Voltammetric experiments were carried out using a CompactStat.e running with IviumSoft 2.124, Ivium Technologies, The Netherlands. The measurements were carried out using a three-electrode system in a 0.5 mL one-compartment electrochemical cell. A glassy carbon (GCE, d = 1.0 mm), a Pt wire, and a Ag/AgCl (3 M KCl) were used as working, auxiliary and reference electrodes, respectively.

The experimental conditions for differential pulse voltammetry (DPV) were: pulse amplitude of 50 mV, pulse width of 100 ms and scan rate of 5 mV s^{-1}. For square wave voltammetry (SWV) a potential increment of 2 mV and pulse amplitude of 50 mV were always used. The frequency and consequently the effective scan rate are indicated in the text.

The GCE was polished using diamond spray, particle size 3 μm (Kemet, UK) before each electrochemical experiment. After polishing, it was rinsed thoroughly with Milli-Q water. Following this mechanical treatment, the GCE was placed in buffer supporting electrolyte and differential pulse voltammograms were recorded until a steady state baseline voltammogram was obtained. This procedure ensured very reproducible experimental results.

2.3 UV-VIS spectrophotometry

Absorption spectra were recorded using a UV-VIS spectrophotometer SPECORD S100 from Carl Zeiss Technology with Win-Aspect software and a 10 mm quartz cuvette. The experimental conditions for absorption spectra were: integration time 25 ms and accumulation 1000 points. All UV-VIS spectra were measured from 200 nm to 400 nm.

2.4 Acquisition and presentation of data

All differential pulse and square wave voltammograms presented were smoothed and baseline-corrected using an automatic function included in the IviumSoft version 2.124. This mathematical treatment improves the visualization and identification of peaks over the baseline without introducing any artefact, although the peak current is in some cases reduced (< 10%) relative to that of the untreated curve. Nevertheless, this mathematical treatment of the original voltammograms was used in the presentation of all experimental voltammograms for a better and clearer identification of the peaks. The values for peak current presented in all graphs were determined from the original untreated voltammograms.

Origin Pro 8.0 from OriginLab Corporation was used for the presentation of all the experimental data reported in this work.

3 Results and discussion

3.1 Cyclic voltammetry

The voltammetric behaviour of danusertib at a clean GCE was initially investigated in the potential range +1.40 V until -1.20 V, by cyclic voltammetry (CV) in 0.1 M phosphate buffer pH = 7.0, in a N_2-saturated solution (not shown). Peaks were observed in the anodic region showing that danusertib undergoes oxidation at the GCE surface. For this reason, all subsequent experiments were carried out in the anodic region.

The oxidation of danusertib was investigated by CV in solutions of 50 μM danusertib in 0.1 M supporting electrolytes with 2.0 < pH < 12.0.

Cyclic voltammograms recorded in a solution of 50 μM danusertib in pH = 3.4 showed three consecutive anodic charge transfer reactions: peak 1_a at E_{p1a} = +0.97 V, peak 2_a at E_{p2a} = +1.03 V and a small peak 3_a at E_{p3a} = +1.22 V, Fig. 1A. Reversing the scan direction, a cathodic peak appeared at E_{pc} = +0.85 V. By recording successive voltammograms in the same solution without cleaning the GCE surface, the decrease of all peaks was due to the adsorption of danusertib oxidation products at the GCE surface, reducing the electroactive area. No additional signal was observed showing that the oxidation products of danusertib are not electroactive.

In order to clarify the origin of the cathodic peak at +0.85 V, two new experiments were carried out in the same solution always with a clean GCE surface. In the first experiment, the scan direction was inverted at +0.96 V, which corresponded to peak 1_a but before occurrence of peak 2_a. No cathodic reaction was observed in these conditions, Fig. 1A. In a new experiment, changing the scan direction at +1.15V, i.e. after the occurrence of peak 2_a but before 3_a, the cathodic correspondent peak 2_c appeared at E_{p2c} = +0.85 V, Fig. 1A.

Also, cyclic voltammograms were recorded in a solution of 50 μM danusertib in pH = 5.7, and peaks 1_a, 2_a and 3_a were observed, Fig. 1B. The potential difference between peaks 1_a and 2_a decreased relative to the voltammogram recorded in solutions with lower pH values, Fig. 1A, hence peaks 1_a and 2_a overlapped. However, after changing the scan direction, the cathodic correspondent peak 2_c appeared. Successive cyclic voltammograms were recorded without cleaning the electrode surface and peak currents decreased.

The effect of scan rate on the oxidation of danusertib was evaluated in pH = 7.0 (not shown). In these conditions, peaks 1_a and 2_a merged and only one anodic peak was observed. Increasing the scan rate the peak potential shifted to more positive values. The peak current

increased but the linear relationship log I_{pa} vs. log v with a slope of -0.75 showed that the oxidation of danusertib involves adsorption of the compound at the GCE surface. Also, an increase of the ratio between the anodic and the cathodic peak currents was observed.

Cyclic voltammograms recorded in solutions of danusertib in supporting electrolytes with different pH values showed that danusertib oxidation is pH-dependent.

3.2 Differential pulse voltammetry

The pH effect on the electrochemical oxidation of danusertib was investigated for electrolytes with 2.0 < pH < 12.0, using different voltammetric techniques. DPV allowed lower detection limits and a better visualisation of all redox processes. DP voltammograms were recorded in solutions of 5 μM danusertib in electrolytes with different pH values, Fig. 2A.

For pH < 5.0, three charge transfer reactions at peak 1_a, 2_a and 3_a were observed, Fig. 2A. The peak potentials were pH dependent and shifted linearly to less positive values with increasing pH, Fig. 2B. For peak 1_a, the relationship was E_{p1a} = 0.97 - 0.03 pH. The slope of the line, -30 mV per pH unit, corresponded to a mechanism in which the number of protons transfer is half of the number of electrons. For peaks 2_a and 3_a, the relationships were E_{p2a} = 1.12 – 0.06 pH and E_{p3a} = 1.48 – 0.06 pH, respectively. The slopes of -60 mV per pH unit were in agreement with oxidation reactions that involved the transfer of the same number of electrons and protons.

For electrolytes with 5.7 < pH < 9.2, only one, pH-dependent peak was observed, Fig. 2A. The width at half height of the peak ($W_{1/2}$) varied between 75 and 80 mV, which is higher than the theoretical value for a system that involves the transfer of 2 electrons but smaller than the value correspondent to 1 electron. The value of $W_{1/2}$ can be explained considering the overlapping of peaks 1_a and 2_a, Fig. 2B, each corresponding to the transfer of two electrons.

For pH > 10.0, peak 1_a appeared at higher potential values than peak 2_a, Fig. 2A. In these conditions, the potential of peak 1_a was pH-independent, Fig. 2B, suggesting an oxidation mechanism that involves only the transfer of electrons after chemical deprotonation. The value of $pK_a \sim 10.0$ of danusertib was determined.

Consecutive DP voltammograms were recorded in solutions of different concentrations and pH values, and after the transfer of the electrode to the supporting electrolyte, Fig. 3.

For pH = 4.5, the voltammogram recorded in 1 μM danusertib showed both peaks 1_a and 2_a, Fig. 3A. By recording successive voltammograms, no additional signal occurred showing that the oxidation products of danusertib are not electroactive. After recording two voltammograms in solution, the electrode was washed with a jet of deionised water and placed in the electrochemical cell containing only buffer. The first voltammogram showed both peaks 1_a and 2_a, Fig. 3A. On the second voltammogram recorded in the same conditions, without cleaning the electrode surface, only a small peak 2_a occurred, Fig. 3A.

A similar experiment has been carried out at pH = 5.7, Fig. 3B. On the first DP voltammogram recorded in 0.1 μM danusertib peaks 1_a and 2_a overlapped, hence one peak occurred. On the second scan in solution without cleaning the GCE surface a better visualisation of both peaks 1_a and 2_a was observed and their currents decreased.

3.3 Square wave voltammetry

In SWV the current is sampled in both positive and negative-going pulses, oxidation and reduction peaks of the electroactive compound can be obtained simultaneously, and the reversibility of the electron transfer reaction monitored by plotting the forward and backward components of the total current.

SW voltammograms were recorded in solutions of 5 μM danusertib in electrolytes with different pH values, Fig. 4.

At pH = 2.0, three peaks 1_a, 2_a and 3_a were observed, Fig. 4A. The forward and backward components of the total current showed peaks corresponding to oxidation at peaks 1_a and 3_a, and to oxidation and reduction at peak 2_a. This experiment confirmed that danusertib oxidation at peaks 1_a and 3_a is irreversible whereas the redox reaction at peak 2_a is reversible.

At pH =12.0, only peaks 2_a and 1_a occurred, Fig. 4B. The deconvolution of the total current showed at peak 2_a unequal values for both current and potential. This can be explained considering that danusertib oxidation at peak 2_a involve the formation of a product that undergoes homogenous chemical reaction. At the same time, the irreversibility of danusertib oxidation at peak 1_a was observed one more time.

3.4 Analytical determination

The analytical determination of danusertib was investigated by SWV and UV-VIS spectrophotometry, Fig. 5 and Table 2.

SW voltammograms were recorded for standard additions of danusertib corresponding to bulk concentrations between 50 and 500 nM in pH = 7.0, Fig. 5A. The detection limit (LOD) was determined as the substance concentration that led to a peak with a height three times the baseline noise level, and was calculated from LOD = 3 × S.D. × (sensitivity)$^{-1}$. Using the equation $I_{pa} = I_{pa}(C_{danusertib})$, the obtained LOD = 27.4 nM, Table 2. The quantification limit (LOQ) is the lowest concentration of a substance that can be quantified with acceptable precision and accuracy. A typical signal/noise ratio of 10 is generally considered to be acceptable; therefore: LOQ = 10 × S.D. × (sensitivity)$^{-1}$. Thus, LOQ = 91.2 nM was determined.

UV-VIS spectra were recorded for standard additions of danusertib corresponding to bulk concentrations between 1 and 10 μM in pH = 7.0, Fig. 5B. Danusertib has shown three absorption bands: at 204, 217 and 301 nm. The well-defined absorption band at 301 nm was used as analytical signal for the determination of the calibration curve. Using the equations $A = A(C_{danusertib})$, LOD = 0.5 μM and LOQ = 1.6 μM were determined.

The reproducibility of these methods was evaluated by plotting different calibration curves. The relative standard deviations (R.S.D.), Table 2, calculated from the sensitivities of three calibration curves were around 5.6 % and 0.5 % for SWV and UV-VIS procedures, respectively. It must be mentioned that each electrochemical measurement was done using a freshly polished GCE, a process that give rise to small modifications of the electrode surface area which can in turn cause variations in the oxidation currents, which was the main source of error in the electrochemical procedure described.

3.5 Oxidation mechanism

The electrochemical oxidation of danusertib in acid media showed three consecutive, pH-dependent charge transfer reactions at peaks 1_a, 2_a and 3_a, Fig. 6A. The potential of peak 1_a is pH dependent and its value increases with the pH following a linear relationship of -30 mV / pH unit. Also, peaks 2_a and 3_a varied with -60 mV / pH unit. The small potential difference between peaks 1_a and 2_a, and their different variations with the pH, allow peaks 1_a and 2_a to overlap in neutral and mild alkaline electrolytes, Fig. 2B. For pH > 10.0, the oxidation at peak 1_a turns pH independent, and peaks 1_a and 2_a occur at distinct potential values, Fig. 2B. The behaviour described is consistent with the existence of three different electroactive centres in the danusertib molecule.

For the determination of danusertib oxidation mechanism, experiments have been carried out in solutions of imatinib mesylate and piperazine citrate, which present similar molecular features with danusertib.

On the first DP voltammogram in a solution of 5 μM imatinib mesylate in pH = 4.5, two consecutive charge transfer reactions were observed at +0.87 V and +1.22 V, Fig. 6B. On the second DP voltammogram, the oxidation product of imatinib appeared at +0.32 V. Previous results have been shown that the oxidation of imatinib is irreversible and involves the formation of an oxidation product that undergoes reversible redox reactions [19,20].

The DP voltammogram recorded in a solution of 5 μM piperazine citrate in pH = 4.5 showed one oxidation peak at +1.23 V, Fig. 6B.

Comparing the voltammetric behaviour of danusertib and imatinib mesylate, Fig. 6A and B, and considering their chemical structures, Schemes 1A and B, an oxidation mechanism of danusertib is proposed. For pH < 10.0, the irreversible oxidation of danusertib at peak 1_a corresponds to the removal of two electrons and one proton from the amide moiety, Scheme 2A. This oxidation reaction results in a nitrenium (aminylium) cation, in agreement with previous reports on the oxidation of amides [27-29]. For pH > 10.0, the amide group undergoes chemical deprotonation and the oxidation involves only the transfer of electrons. The oxidation of imatinib is similar, but the formation of a quinone structure [19,20] at the aromatic ring in the vicinity of the amide group, Scheme 1B, explains the occurrence of the oxidation product observed in the solution of imatinib, Fig. 6A. In the case of danusertib, this aromatic ring is absent, Scheme 1A, and no electroactive oxidation product was observed, Fig. 6A, hence the oxidation product of danusertib undergoes a chemical reaction. It is proposed that the nitrenium cation reacts with water in agreement with previous results [30,31], resulting in a *N*-hydroxy amide derivative, Scheme 1A. On the other hand, the small

difference (~ 40 mV) between the oxidation peaks of danusertib and imatinib, Fig. 6A and B, is due to steric effects imposed by the uncommon moieties in their structures.

The voltammograms in the solution of danusertib in acid media show the reversible charge transfer reaction at peak 2_a, Fig. 4A and 6A, which does not not occur in solutions of imatinib, Fig. 6B. It is proposed that this reaction is due to the transfer of two electrons and two protons from the pyrrolo-pyrazol moiety, Scheme 2B, with the formation of an oxidation product that undergoes reaction with water in alkaline electrolytes, Fig. 4B and Scheme 2B.

For peak 3_a of danusertib, Fig. 6A and B, it is proposed that the oxidation involves the piperazine moiety. The redox behaviour of piperazine containing compounds has been previously reported [22-26]. Considering that in acid media piperazine moiety is protonated (pK_{a1} ~ 7 and pK_{a2} ~ 3), the electrochemical oxidation of danusertib at peak 3_a occurs with the transfer of two electrons and two protons from the nitrogen atom in the proximity of the methyl group leading to the formation of iminium cation, Scheme 2C, which is hydrolysed forming an amine derivative and formaldehyde [26].

4 Conclusion

The electrochemical oxidation mechanism of the anti-cancer drug and kinase inhibitor danusertib has been studied at a glassy carbon electrode by cyclic, differential pulse and square wave voltammetry. Three consecutive, pH-dependent charge transfer reactions were observed in electrolytes with pH values correspondent to acid media. For neutral and alkaline electrolytes one or two oxidation peaks occurred, respectively. The number of electrons and protons involved in each step of danusertib oxidation mechanism, and the value of pKa ~ 10.0 were calculated.

The analytical determination of danusertib was carried out by square wave voltammetry and UV-VIS spectrophotometry at 0.1 M phosphate buffer pH = 7.0. The

detection limits were 27.4 nM and 0.5 μM, respectively. The limits of quantification were calculated and the reproducibility of the methods was also evaluated.

The investigation of compounds with similar structures such as imatinib mesylate and piperazine citrate allowed the identification of danusertib electroactive centres and a redox mechanism of danusertib was proposed.

Acknowledgment

Financial support from: Fundação para a Ciência e Tecnologia (FCT) under the projects PTDC/SAU-BEB/104643/2008, PTDC/DTP-FTO/0191/2012, and PEst-C/EME/UI0285/2013 POCI 2010 (co-financed by the European Community Fund FEDER), FEDER funds through the program COMPETE – Programa Operacional Factores de Competitividade, QREN – Quadro de Referência Estratégico Nacional Portugal 2007.2013 – programa Mais Centro through the project MT4MOBY, and CEMUC-R (Research Unit 285), is gratefully acknowledged.

References

[1] N. Dhanasekaran, E.P. Reddy, Signaling by dual specificity kinases, Oncogene 17 (1998) 1447.

[2] J.A. Ubersax, J.E. Ferrell Jr., Mechanisms of specificity in protein phosphorylation, Nat. Rev. Mol. Cell Biol. 8 (2007) 530.

[3] G. Vader, S.M.A. Lens, The Aurora kinase family in cell division and cancer, Biochim. Biophys. Acta 1786 (2008) 60.

[4] M. Kollareddy, P. Dzubak, D. Zheleva, M. Hajduch, Aurora kinases: structure, functions and their association with cancer, Biomed. Pap. 152 (2008) 27.

[5] M.E.M. Noble, J.A. Endicott, L.N. Johnson, Protein Kinase Inhibitors: Insights into Drug Design from Structure, Science 303 (2004) 1800.

[6] T. Ikezoe, Aurora kinases as an anti-cancer target, Cancer Lett. 262 (2008) 1.

[7] J.J.E.M. Kitzen, M.J.A. de Jonge , J. Verweij, Aurora kinase inhibitors, Crit. Rev. Oncol. Hematol. 73 (2010) 99.

[8] D. Fancelli, J. Moll, M. Varasi, R. Bravo, R. Artico, D. Berta, S. Bindi, A. Cameron, I. Candiani, P. Cappella, P. Carpinelli, W. Croci, B. Forte, M.L. Giorgini, J. Klapwijk, A. Marsiglio, E. Pesenti, M. Rocchetti, F. Roletto, D. Severino, C. Soncini, P. Storici, R. Tonani, P. Zugnoni, P. Vianello, 1, 4, 5, 6-tetrahydropyrrolo[3, 4-c]pyrazoles: identification of a potent Aurora kinase inhibitor with a favorable antitumor kinase inhibition profile, J. Med. Chem. 49 (2006) 7247.

[9] P. Carpinelli, R. Ceruti, M.L. Giorgini, P. Cappella, L. Gianellini, V. Croci, A. Degrassi, G. Texido, M. Rocchetti, P. Vianello, L. Rusconi, P. Storici, P. Zugnoni, C. Arrigoni, C. Soncini, C. Alli, V. Patton, A. Marsiglio, D. Ballinari, E. Pesenti, D. Fancelli, J. Moll, PHA-739358, a potent inhibitor of Aurora kinases with a selective target inhibition profile relevant to cancer, Mol. Cancer Ther. 6 (2007) 3158.

[10] N. Steeghs, F.A.L.M. Eskens, H. Gelderblom, J. Verweij, J.W.R. Nortier, J. Ouwerkerk, C. van Noort, M. Mariani, R. Spinelli, P. Carpinelli, B. Laffranchi, M.J.A. de Jonge, Phase I Pharmacokinetic and Pharmacodynamic Study of the Aurora Kinase Inhibitor Danusertib in Patients With Advanced or Metastatic Solid Tumors, Clin. Oncol. 27 (2009) 5094.

[11] N. Steeghs, R.H.J. Mathijssen, J.A.M. Wessels, A.-J. de Graan, T. van der Straaten, M. Mariani, B. Laffranchi, S. Comis, M.J.A. de Jonge, H. Gelderblom, H.-Jan Guchelaar, Influence of pharmacogenetic variability on the pharmacokinetics and toxicity of the aurora kinase inhibitor danusertib, Invest. New Drugs 29 (2011) 953.

[12] A. Gontarewicz, T.H. Brummendorf, Danusertib (formerly PHA-739358) - a novel combined pan-Aurora kinases and third generation Bcr-Abl tyrosine kinase inhibitor, Recent Results Cancer Res. 184 (2010) 199.

[13] H.J. Meulenbeld, J.P. Bleuse, E.M. Vinci, E. Raymond, G. Vitali, A. Santoro, L. Dogliotti, R. Berardi, F. Cappuzzo, S.T. Tagawa, C.N. Sternberg, M.G. Jannuzzo, M. Mariani, A. Petroccione, R. de Wit, Randomized phase II study of danusertib in patients with metastatic castration-resistant prostate cancer after docetaxel failure, BJU Int. 111 (2013) 44.

[14] K. Fraedrich, J. Schrader, H. Ittrich, G. Keller, A. Gontarewicz, V. Matzat, A. Kromminga, A. Pace, J. Moll, M. Blaker, A.W. Lohse, D. Horsch, T.H. Brummendorf, D. Benten, Targeting aurora kinases with danusertib (PHA-739358) inhibits growth of liver metastases from gastroenteropancreatic neuroendocrine tumors in an orthotopic xenograft model, Clin. Cancer Res. 18 (2012) 4621.

[15] D. Benten, G. Keller, A. Quaas, J. Schrader, A. Gontarewicz, S. Balabanov, M. Braig, H. Wege, J. Moll, A.W. Lohse, T.H. Brummendorf, Aurora kinase inhibitor PHA-739358

suppresses growth of hepatocellular carcinoma in vitro and in a xenograft mouse model, Neoplasia 11 (2009) 934.

[16] F.P.S. Santos, FPS A. Quintas-Cardama, New drugs for chronic myelogenous leukemia, Curr. Hmeatol. Malig. Rep. 6 (2011) 96.

[17] H.J. Meulenbeld, R.H. Mathijssen, J. Verweij, R. de Wit, M.J. de Jonge, Danusertib, an aurora kinase inhibitor, Expert Opin. Investig. Drugs 21 (2012) 383.

[18] M. Modugno, E. Casale, C. Soncini, P. Rosettani, R. Colombo, R. Lupi, L. Rusconi, D. Fancelli, P. Carpinelli, A.D. Cameron, A. Isacchi, J. Moll, Crystal Structure of the T315I Abl Mutant in Complex with the Aurora Kinases Inhibitor PHA-739358, Cancer Res. 67 (2007) 7987.

[19] V.C. Diculescu, M. Vivan, A.M. Oliveira Brett, Voltammetric behavior of antileukemia drug glivec. Part I - Electrochemical study of glivec, Electroanalysis 18 (2006) 1800.

[20] V.C. Diculescu, M. Vivan, A.M. Oliveira Brett, Voltammetric behavior of antileukemia drug glivec. Part II - Redox processes of glivec electrochemical metabolite, Electroanalysis 18 (2006) 1808.

[21] V.C. Diculescu, M. Vivan, A.M. Oliveira Brett, Voltammetric behavior of antileukemia drug glivec. Part III: In situ DNA oxidative damage by the glivec electrochemical metabolite, Electroanalysis 18 (2006) 1963.

[22] B. Uslu, B. Dogan, S.A. Ozkan, H.Y. Aboul-Enein, Electrochemical behavior of vardenafil on glassy carbon electrode: Determination in tablets and human serum, Anal. Chim. Acta 552 (2005) 127.

[23] D. Kul, M. Gumustas, B. Uslu, S.A. Ozkan, Electroanalytical characteristics of antipsychotic drug ziprasidone and its determination in pharmaceuticals and serum samples on solid electrodes, Talanta 82 (2010) 286.

[24] S.A. Ozkan, B. Uslu, P. Zuman, Electrochemical oxidation of sildenafil citrate (Viagra) on carbon electrodes, Anal. Chim. Acta 501 (2004) 227.

[25] J.-M. Kauffmann, J.-C. Vire, G.J. Patriarche, 644-Tentative correlation between the electrochemical oxidation of neuroleptics and their pharmacological properties, Bioelectrochem. Bioenerg. 12 (1984) 413.

[26] R.N. Hegde, R.R. Hosamani, S.T. Nandibewoor, Voltammetric oxidation and determination of cinnarizine at glassy carbon electrode modified with multi-walled carbon nanotubes, Colloids Surf. B Biointerfaces 72 (2009) 259-265.

[27] M.J. Legorburu, R.M. Alonso, R.M. Jimenez, Voltammetric study of the diuretic xipamide, Bioelectrochem. Bioenerg. 32 (1993) 57.

[28] K.D. Moeller, Synthetic Applications of Anodic Electrochemistry, Tetrahedron 56 (2000) 9527.

[29] E. Steckhan, Anodic oxidation of nitrogen-containing compounds, in: H. Lund, O. Hammerich (Eds.), Organic Electrochemistry, Mercel Dekker, New York, 2001, p. 545.

[30] T.L. Gilchrist, 6.1 - Oxidation of Nitrogen and Phosphorus, in: B.M. Trost, I. Fleming (Eds.), Comprehensive Organic Synthesis, Pergamon, Oxford, 1991, 735.

[31] S. Srivastava, M. Kercher, D.E. Falvey, On the solution chemistry of parent nitrenium ion NH_2^+: the role of the singlet and triplet states in its reactions with water, methanol, and hydrocarbons, J. Org. Chem. 64 (1999) 5853-5857.

Table 1. Supporting electrolytes, 0.1 M ionic strength.

pH	Composition
2.0	HCl + KCl
3.4	HAcO+NaAcO
4.5	HAcO+NaAcO
5.7	HAcO+NaAcO
6.0	HAcO+NaAcO
7.0	NaH_2PO_4+Na_2HPO_4
8.0	NaH_2PO_4+Na_2HPO_4
9.2	NaH_2PO_4+Na_2HPO_4
10.2	NH_3+NH_4Cl
12.0	NaOH + KCl

Table 2 - Sensitivities, intercepts, limits of detection, limits of quantification and other linear fit parameters calculated from danusertib calibration curves obtained by square wave voltammetry (SWV), Fig. 5A, and by UV-VIS spectrophotometry, Fig. 5B.

method	**sensitivity**	**intercept**	**LOD**	**LOQ**	**R^2**	**S.D.**	**R.S.D.**
SWV	0.099±0.002 nA/nM	-3.789±0.646 nA	27.4 nM	91.2 nM	0.997	0.903 nA	5.4 %
UV-VIS	0.024±0.001 a.u./µM	0.001±0.002 a.u.	0.5 µM	1.6 µM	0.996	0.004 a.u.	0.5 %

Schemes and Figures

Scheme 1 – Chemical structure of: **A)** danusertib and **B)** imatinib mesylate.

Scheme 2 – Proposed oxidation mechanisms of danusertib at different electroactive groups: **A)** amide at peak 1_a, **B)** pyrrolo-pyrazol at peak 2_a and **C)** piperazine at peak 3_a.

Fig. 1 – Cyclic voltammograms in 50 μM danusertib in pH: **A)** 3.4, recorded between +0.00 V and: +1.50 V (black) first and (dotted black) second scans, (red) +0.96 V, and (grey) +1.15 V, and **B)** 5.7, (black) first and (dotted black) second scans; v = 100 mV s^{-1}.

Fig. 2 – **A)** 3-D plot of DP voltammograms base-line corrected in 5 μM danusertib function of pH of the supporting electrolyte. **B)** Plot of E_{pa} of peak (■) 1_a, (●) 2_a and (★) 3_a vs. pH.

Fig. 3 – DP voltammograms base-line corrected in solutions of danusertib: **A)** 1 μM in pH = 4.5 (black) first and (dotted black) second scans in solution, and (red) first and (dotted red) second scans after transferring the electrode to the supporting electrolyte, and **B)** 0.1 μM in pH = 5.7 (black) first and (dotted black) second scans in solution.

Fig. 4 – SW voltammograms base-line corrected in 5 μM danusertib in pH: **A)** 2.0 and **B)** 12.0; I_t, I_f and I_b – total, forward and backward currents, f = 25 Hz, ΔE_s = 2 mV for v = 50 mV s^{-1}.

Fig. 5 - A) SW voltammograms in 0.05, 0.10, 0.15, 0.20, 0.25, 0.30, 0.35, 0.40, 0.45 and 0.50 μM and **B)** UV spectra in 1, 2, 3,4, 5, 6, 7, 8, 9, 10 μM danusertib in pH = 7.0; s.e. represents the voltammogram recorded in buffer; the absorbance and the peak current increase with solution concentration, respectively. For SW voltammetry: f = 10 Hz, ΔE_s = 2 mV for v = 20 mV s^{-1}.

Fig. 6 - DP voltammograms base-line corrected in 5 μM: **A)** danusertib (black) first and (dotted) second scans, and **B)** imatinib mesylate (black) first and (dotted) second scans and (red) piperazine citrate, in pH = 4.5.

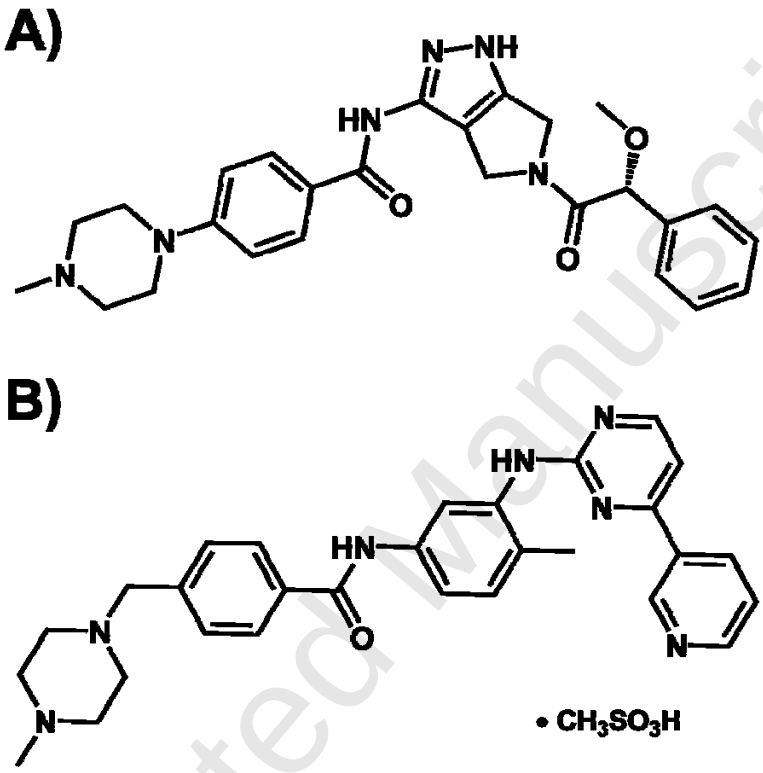

Scheme 1 – Chemical structure of: **A)** danusertib and **B)** imatinib mesylate.

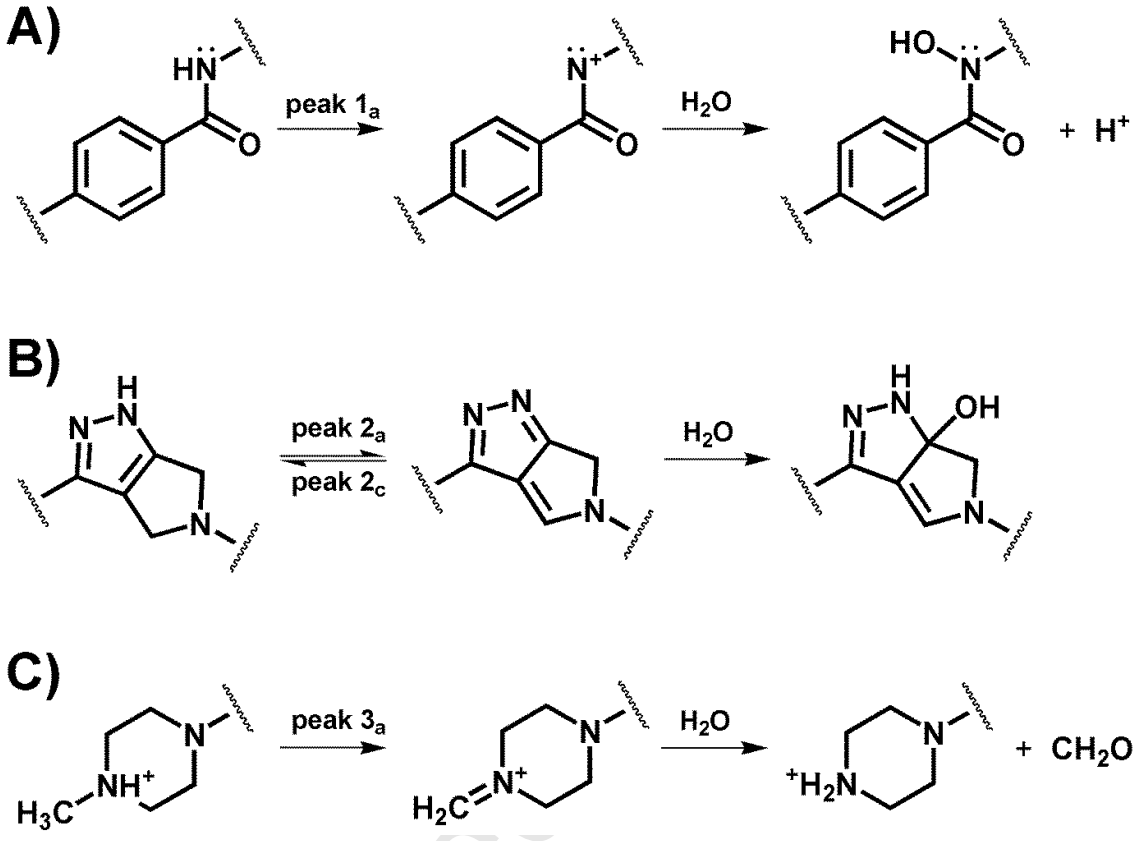

Scheme 2 – Proposed oxidation mechanisms of danusertib at different electroactive groups:

A) amide at peak 1_a, **B)** pyrrolo-pyrazol at peak 2_a and **C)** piperazine at peak 3_a.

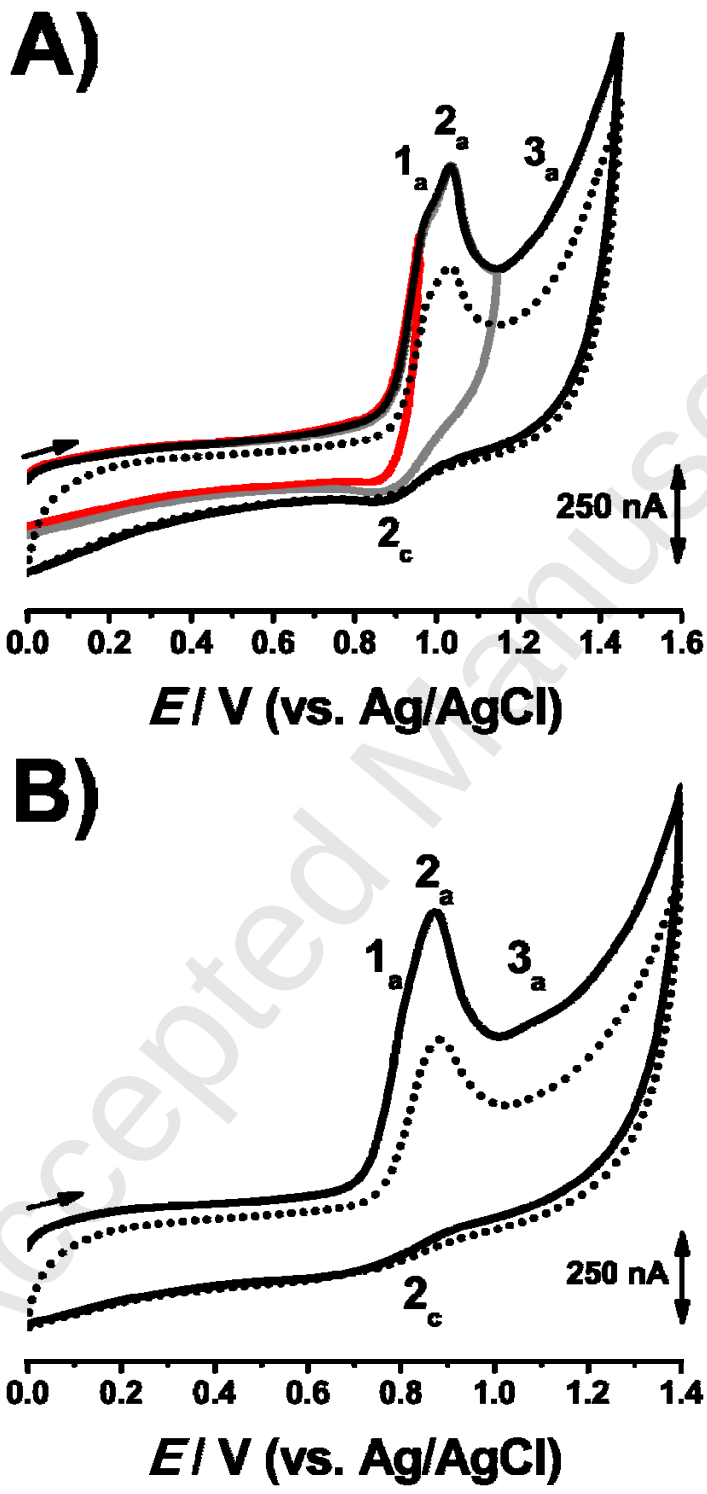

Fig. 1 – Cyclic voltammograms in 50 μM danusertib in pH: **A)** 3.4, recorded between +0.00 V and: +1.50 V (black) first and (dotted black) second scans, (red) +0.96 V, and (grey) +1.15 V, and **B)** 5.7, (black) first and (dotted black) second scans; ν = 100 mV s^{-1}.

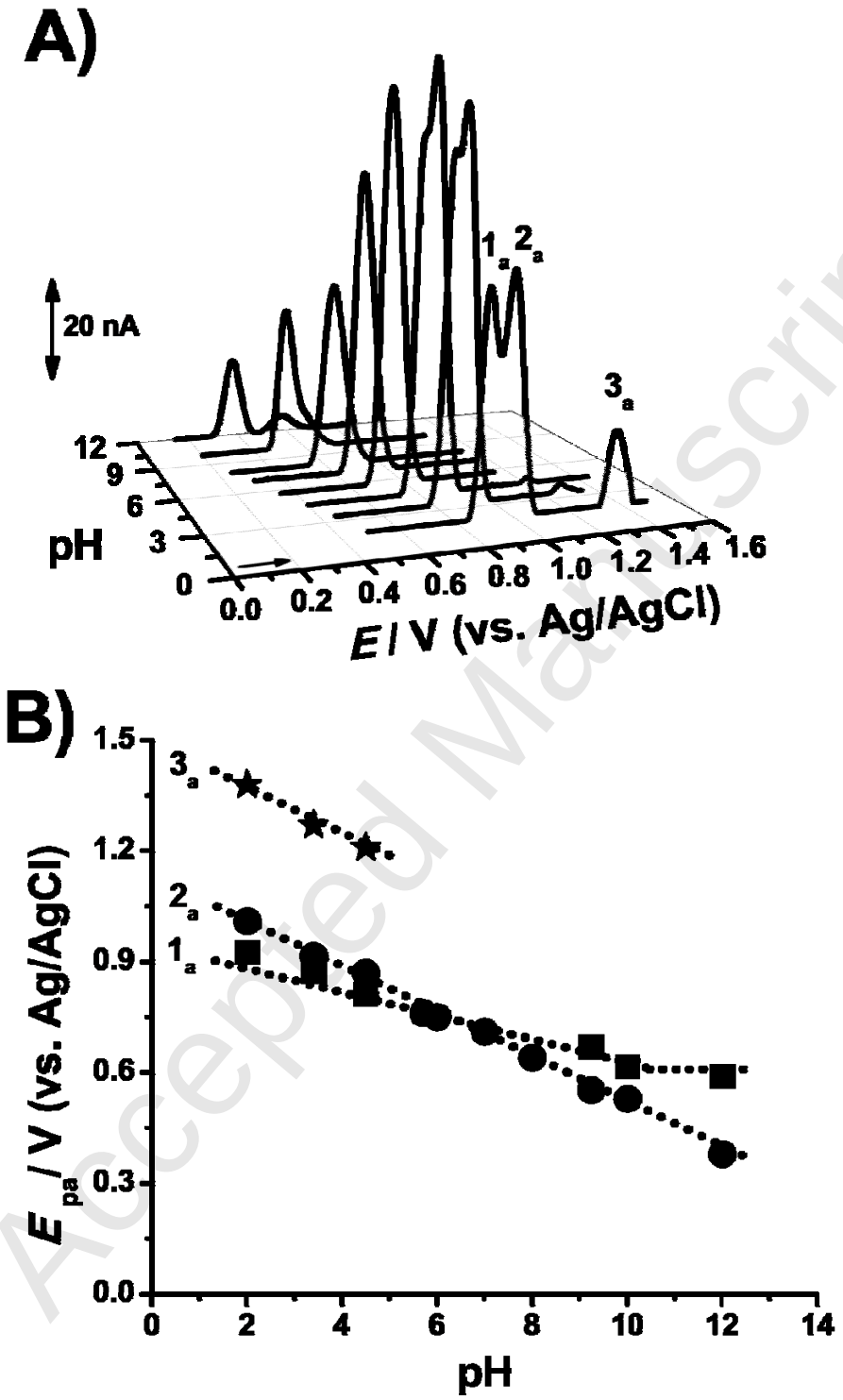

Fig. 2 – **A)** 3-D plot of DP voltammograms base-line corrected in 5 μM danusertib function of pH of the supporting electrolyte. **B)** Plot of E_{pa} of peak (■) 1_a, (●) 2_a and (★) 3_a vs. pH.

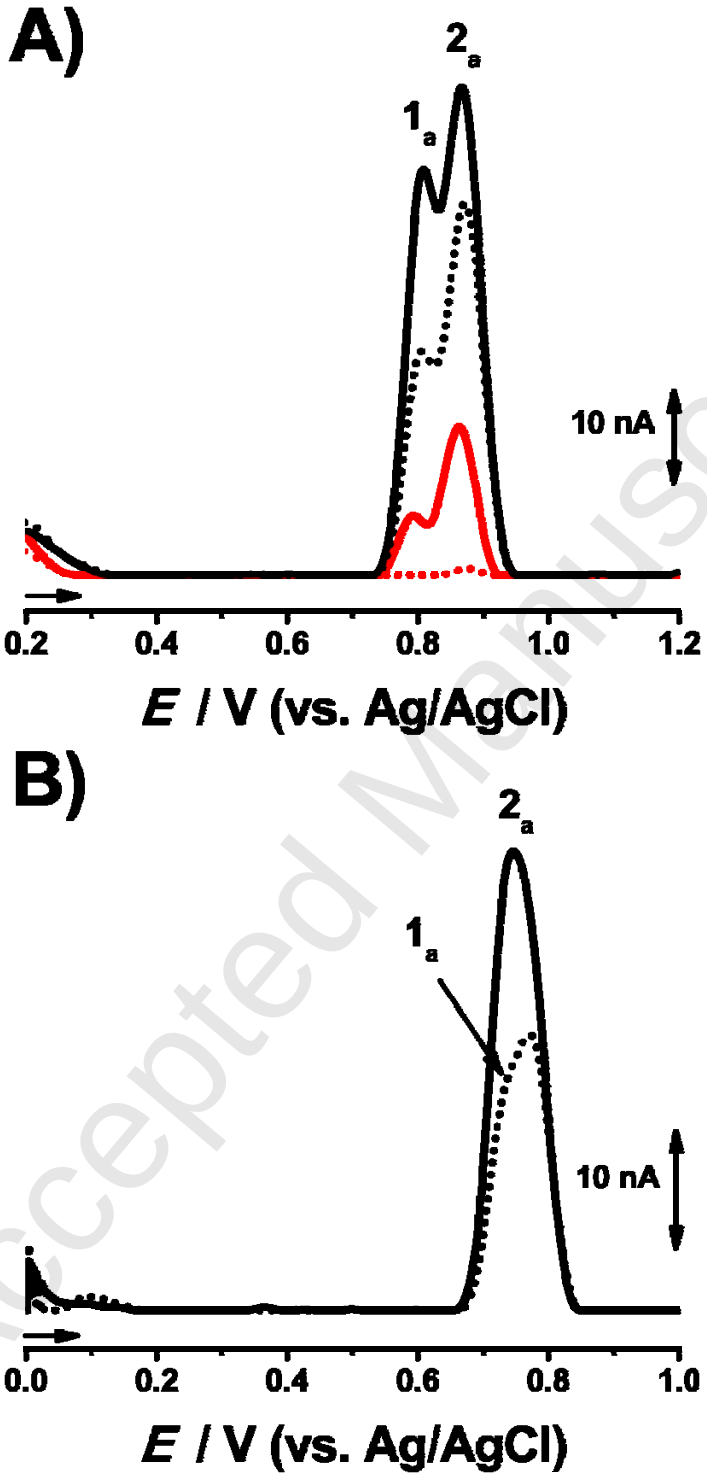

Fig. 3 – DP voltammograms base-line corrected in solutions of danusertib: **A)** 1 μM in pH = 4.5 (black) first and (dotted black) second scans in solution, and (red) first and (dotted red) second scans after transferring the electrode to the supporting electrolyte, and **B)** 0.1 μM in pH = 5.7 (black) first and (dotted black) second scans in solution.

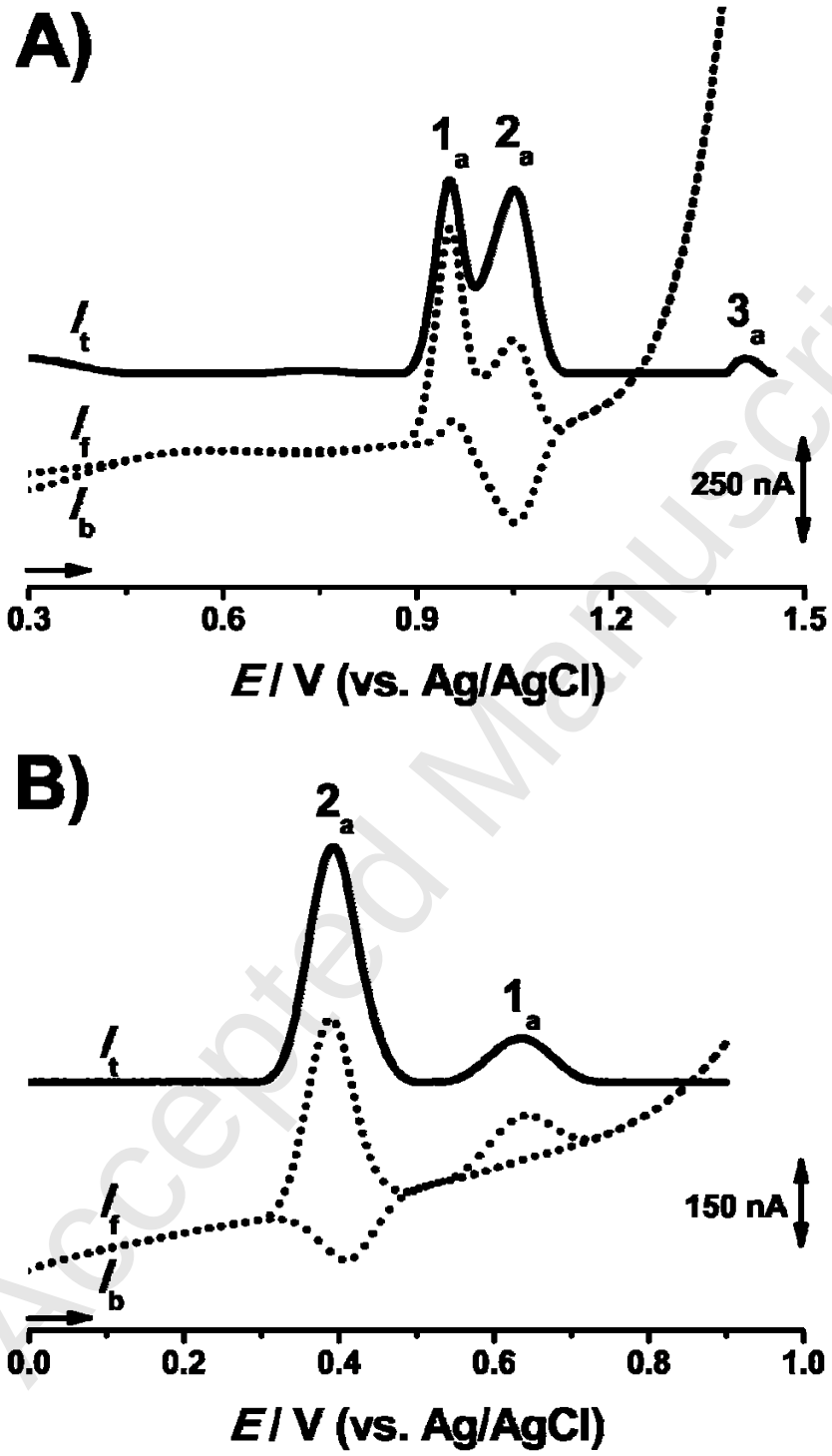

Fig. 4 – SW voltammograms base-line corrected in 5 μM danusertib in pH:

A) 2.0 and **B)** 12.0; I_t, I_f and I_b – total, forward and backward currents,

f = 25 Hz, ΔE_s = 2 mV for v = 50 mV s^{-1}.

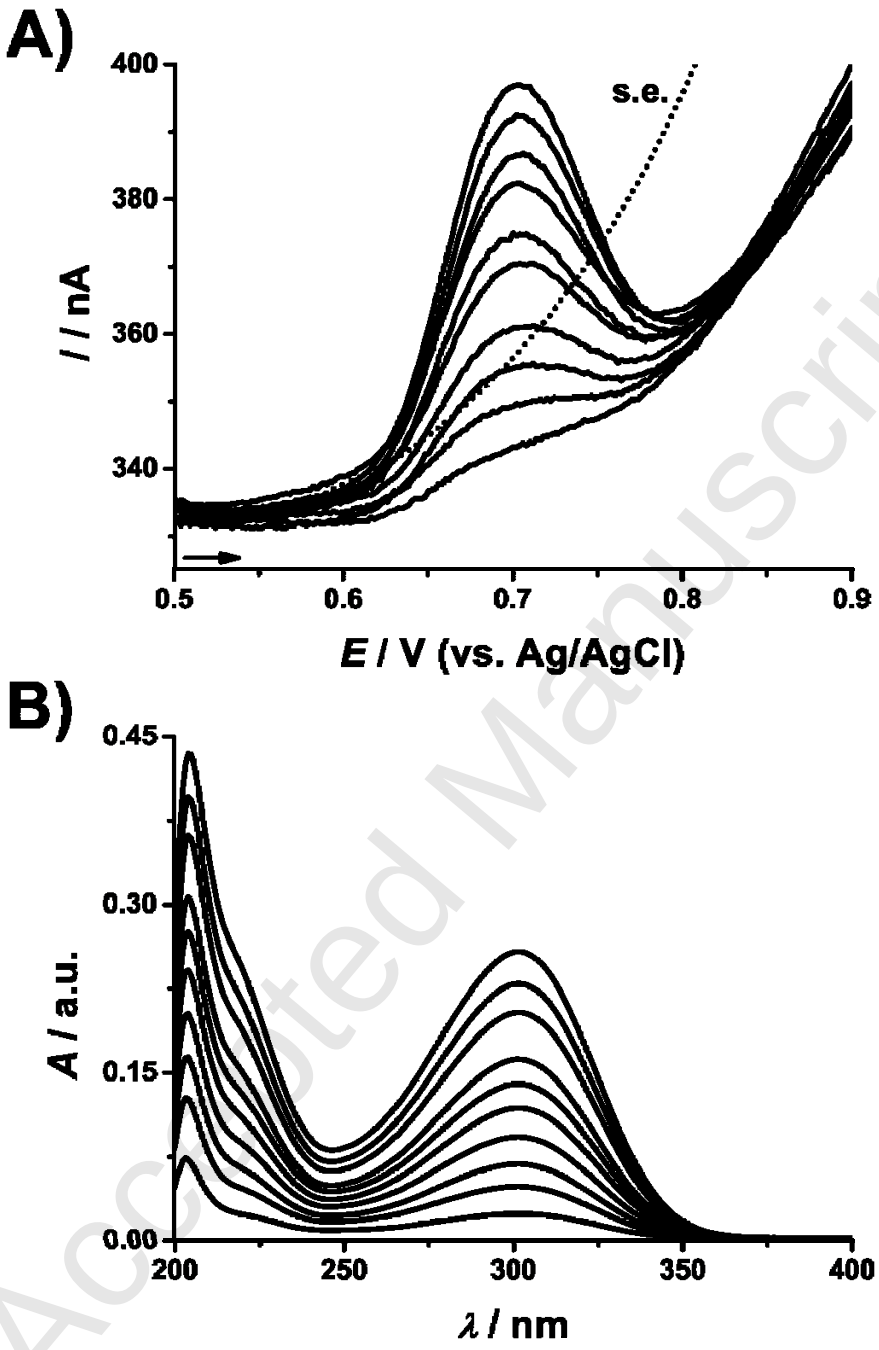

Fig. 5 - A) SW voltammograms in 0.05, 0.10, 0.15, 0.20, 0.25, 0.30, 0.35, 0.40, 0.45 and 0.50 μM and **B)** UV spectra in 1, 2, 3,4, 5, 6, 7, 8, 9, 10 μM danusertib in pH = 7.0;

s.e. represents the voltammogram recorded in buffer;

the absorbance and the peak current increase with solution concentration, respectively.

For SW voltammetry: f = 10 Hz, ΔE_s = 2 mV for v = 20 mV s^{-1}.

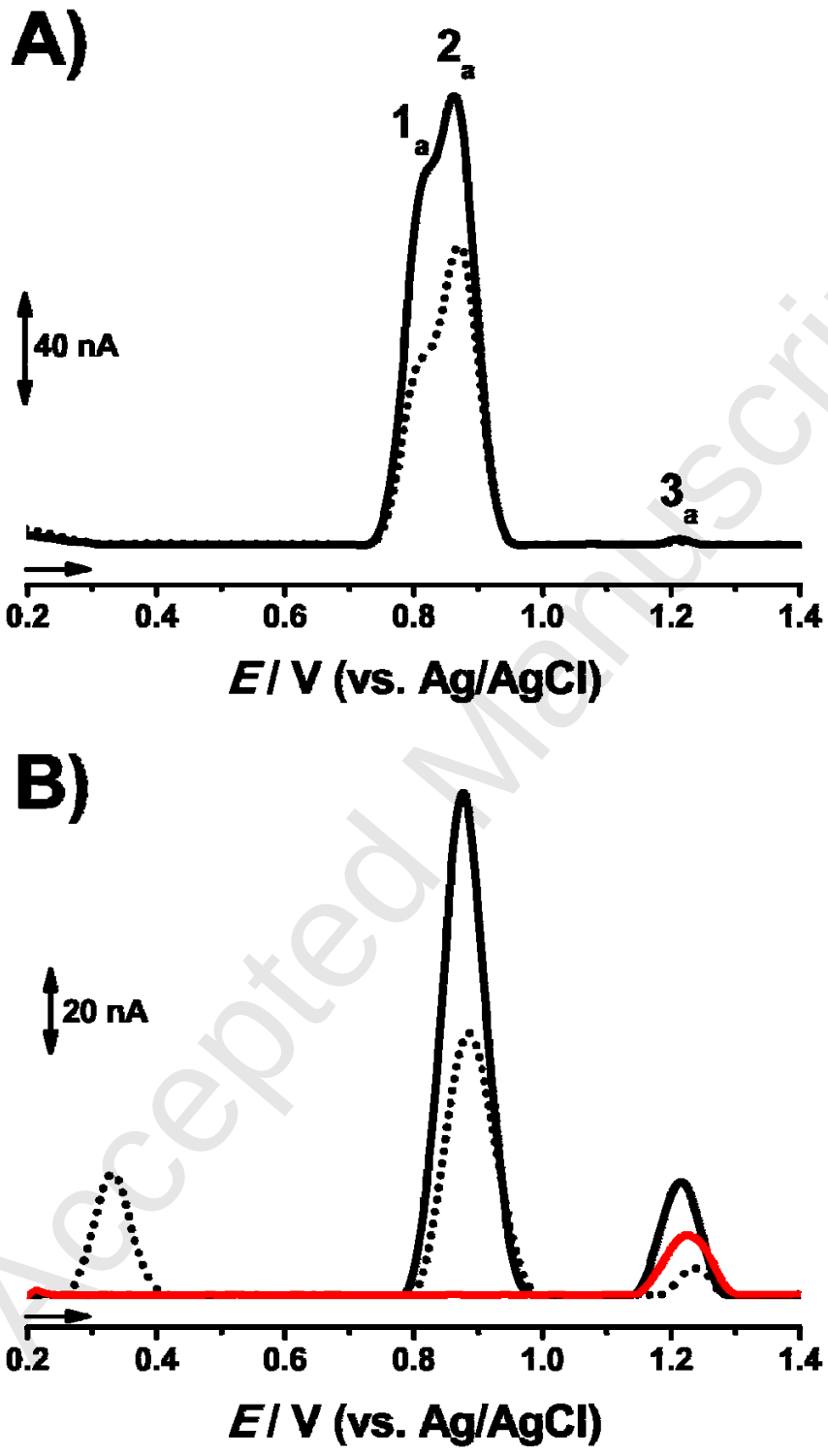

Fig. 6 - DP voltammograms base-line corrected in 5 μM: **A)** danusertib (black) first and (dotted) second scans, and **B)** imatinib mesylate (black) first and (dotted) second scans and (red) piperazine citrate, in pH = 4.5.

GRAPHICAL ABSTRACT

Electrochemical and spectrophotometric characterisation of protein kinase inhibitor and anticancer drug danusertib

Oana M. Popa and Victor C. Diculescu

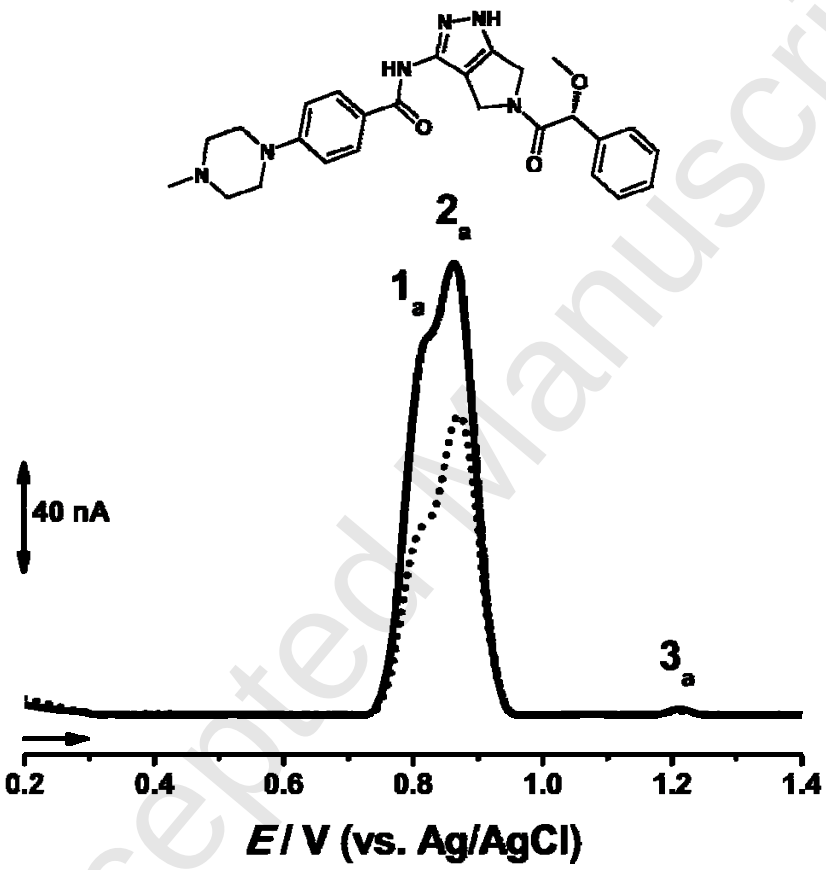

Chemical structure of danusertib and DP voltammograms recorded in

5 μM danusertib in pH = 4.5: (black curve) first and (dotted curve) second scans.

HIGHLIGHTS

clarify the redox mechanism of danusertib;

pH dependent process investigated at a glassy carbon electrode;

number of electrons and protons determined;

analytical determination of danusertib by voltammetry and spectrophotometry;

different electroactive centres identified and redox mechanism proposed.